Eur J Nucl Med Mol Imaging (2011) 38:2005–2013
DOI 10.1007/s00259-011-1875-0

ORIGINAL ARTICLE

Focal uptake of ^{68}Ga-DOTATOC in the pancreas: pathological or physiological correlate in patients with neuroendocrine tumours?

Akram Al-Ibraheem · Ralph Alexander Bundschuh · Johannes Notni · Andreas Buck · Anna Winter · Hans-Jürgen Wester · Markus Schwaiger · Klemens Scheidhauer

Received: 24 March 2011 / Accepted: 26 June 2011 / Published online: 27 July 2011

Abstract
Purpose Neuroendocrine tumours are frequently located in the upper abdomen and especially in the pancreas. Imaging of the abdomen with somatostatin analogs such as ^{68}Ga-DOTA-Phe^{1}-Tyr^{3}-octreotide (DOTATOC) is a standard approach for imaging neuroendocrine cancer, but is still challenging due to physiological and technical considerations in this area. Therefore, the aim of this study was to further investigate the origin of ^{68}Ga-DOTATOC findings in the pancreas.
Methods Forty-three consecutive patients with neuroendocrine tumours were examined by ^{68}Ga-DOTATOC positron emission tomography (PET)/CT for staging or restaging. As imaging of the upper abdomen is frequently affected by breathing artefacts, PET and CT data were analysed for misalignment and rearranged if necessary. Any noticeable uptake in the pancreas was described. Tracer uptake in the head of the pancreas and the liver was measured by means of maximum and average standard uptake value (SUV_{max}, SUV_{av}). The reference standards (malignant versus benign) for correlation with PET findings were clinical and radiological follow-up (mean follow-up time 14 months) (n=37) or histological confirmation (n=6).
Results In 23 of 43 studies (54%) misalignment between PET and CT data was found with a mean value of 1.4 cm. Visual assessment demonstrated that 20 of 43 scans (46.6%) showed no uptake in the head of the pancreas. Of 43 scans, 23 (53.4%) showed noticeable uptake with focal pattern in the head of the pancreas in 10 scans and irregular pattern in 13 scans. Follow-up indicated malignant pancreatic lesions in three patients. The pancreatic head to liver SUV_{av} ratios in these patients ranged from 1.62 to 6.85, whereas in cases of uptake without known malignancy ratios ranged from 0.56 to 1.19. Considering SUV_{max}, the ratio ranged from 3.24 to 9.1 and from 0.84 to 1.47, respectively. No statistically significant difference was noted between uptake in the head of the pancreas and the liver in patients without malignant pancreatic tumours (p>0.05).
Conclusion ^{68}Ga-DOTATOC uptake in the head of the pancreas is a common finding in patients undergoing ^{68}Ga-DOTATOC PET/CT. However, this finding most likely represents a physiological condition, especially if the uptake in the pancreatic head is similar to the uptake in the liver (uptake ratio head to liver SUV_{av}<1.4). Therefore, quantification is recommended to avoid false-positive diagnosis. Misalignment due to respiratory motion must always be taken into account.

Keywords ^{68}Ga-DOTATOC · Neuroendocrine tumour · Head of pancreas · Liver · SUV

A. Al-Ibraheem · R. A. Bundschuh (✉) · J. Notni · A. Buck · A. Winter · H.-J. Wester · M. Schwaiger · K. Scheidhauer
Nuklearmedizinische Klinik und Poliklinik,
Klinikum rechts der Isar der Technischen Universität München,
Ismaninger Str. 22,
81675 Munich, Germany
e-mail: ralph.bundschuh@tum.de

A. Al-Ibraheem
Department of Radiology and Nuclear Medicine,
King Hussein Cancer Center,
Amman, Jordan

A. Buck
Nuklearmedizinische Klinik und Poliklinik,
Universitätsklinikum Würzburg,
Wuerzburg, Germany

Introduction

Imaging of somatostatin receptor (SSTR)-expressing tumours has been greatly improved by the use of combined

positron emission tomography/computed tomography (PET/CT) using the ^{68}Ga-labelled somatostatin analog DOTA-D-Phe^{1}-Tyr^{3}-octreotide (DOTATOC) as the tracer. Numerous reports have recently demonstrated the superiority over other PET tracers such as ^{18}F-fluorodeoxyglucose (FDG) as well as established tracers for planar scintigraphy and single photon emission computed tomography (SPECT) imaging, including ^{111}In-diethylenetriaminepentaacetic acid (DTPA)-octreotide. Also sensitivity for neuroendocrine cancers has been described to be superior to anatomically based imaging modalities such as CT and MRI [5, 7, 9–11, 13, 17, 18].

The upper abdomen and especially the pancreas are frequent manifestation sites of (primary) neuroendocrine tumours. Imaging of the pancreas with radiolabelled somatostatin analogs is challenging since up to 90% of α- and β-cells in normal human pancreas show at least some physiological SSTR2–5 expression [12], reducing the specificity of functional imaging in this area. Moreover, the area of the upper abdomen and especially the head of the pancreas are subject to various sources of artefacts during PET/CT interpretation, in particular due to misregistration of PET and CT data originating from respiratory motion and physiological hepatobiliary excretion of the radiopharmaceutical compound. Strong respiratory movement found in the upper abdomen [2] can influence the qualitative and quantitative analysis of the PET images [15]. Due to misalignment between the CT images and the PET images which are acquired in different breathing states (average over many breathing cycles in PET and snapshot of one breathing state in CT) PET findings may be assigned to wrong anatomical locations [4]. Therefore, the aim of this study was to further investigate the origin of ^{68}Ga-DOTATOC uptake in the pancreas.

Materials and methods

Patients

A total of 77 consecutive ^{68}Ga-DOTATOC PET/CT scans of 59 patients with a diagnosis of neuroendocrine tumours were taken into account for this study. Exclusion criteria included prior surgery or radiation therapy of the pancreatic region, follow-up period less than 6 months or missing follow-up data, and known disseminated liver metastases to avoid activity spillover from from metastases close to the pancreas: for further evaluation 43 patients (age range 28–81 years, mean 64) could be included. The location and prevalence of primary malignancies are given in Table 1. The mean post-imaging follow-up was 14 months (range 6–20 months). The reference standards (malignant versus benign) for correlation with PET findings were clinical and radiological follow-up including the specific tumour markers, ultrasound and CT scan in all patients, and ^{68}Ga-DOTATOC PET in six patients and histological confirmation in six patients. In case of unclear findings in conventional imaging endosonography was performed.

Table 1 Location and prevalence of primary malignancies

Type	Location	Number
Carcinoid	Small bowel	10
	Lung	6
	Stomach & duodenum	5
	Large bowel	4
	Appendix	3
	Thyroid	3
	Pancreas	3
	Unknown	9

Radiopharmaceutical

Labelling

^{68}Ga-DOTATOC was prepared on a fully automated system (GallElute, Scintomics, Fürstenfeldbruck, Germany). A ^{68}Ge/^{68}Ga generator with SnO_2 matrix (obtained from iThemba LABS, Cape Town, South Africa) was eluted with 1.0 M HCl, prepared from 30% HCl and water (both Merck Ultrapur). A fraction of 1.25 ml containing the highest activity (ca. 1.1–1.3 GBq) was transferred into a standard reactor vial (Alltech, 5 ml) containing a solution of 20 μg DOTATOC (Bachem) and 600 mg hydroxyethylpiperazine ethanesulfonic acid (HEPES) (Merck) in 0.5 ml water, resulting in a pH of 3.2–3.3. The vial was heated to 95°C for 5 min while air was slowly bubbled through the solution for agitation. Then the mixture was passed over a fixation cartridge (Sep-Pak Classic C18, sorbent amount of 100 mg) that was previously conditioned by purging with 5 ml of ethanol (absolute, Ph. Eur.) and 10 ml of water. The cartridge was purged with 10 ml of water and air. ^{68}Ga-DOTATOC was eluted from the cartridge with 1 ml of ethanol followed by purging with 10 ml of phosphate-buffered saline (PBS) buffer (pH 7.4) and passed through a 0.22-μm filter (Millex GV, Millipore) directly into a sterile vial (CisBio), yielding 700–800 MBq of formulated ^{68}Ga-DOTATOC after 20 min.

Quality control

Radio-thin layer chromatography (TLC) of the product was performed using ITLC-SG plates (Pall Life Sciences, Ann Arbor, MI, USA) using two eluent systems, 0.1 M sodium citrate in water (TLC1) and a 1:1 (v/v) mixture of an aqueous solution of 1.0 M sodium acetate and methanol

(TLC2). For TLC1, free $^{68}Ga^{3+}$ is eluted with the solvent front (R_F ca. 1) and the product stays at the origin (R_F=0), whereas for TLC2 the product is eluted (R_F of 0.6–0.8) and all ^{68}Ga impurities are retained at the origin (R_F=0). Purity determined by either method was always better than 99%. Radio-HPLC was performed on a Sykam system using a Chromolith column (Merck, 100×4.6 mm) with radioactivity and UV detection (220 nm). Eluents were water (A) and acetonitrile (B), both containing 0.1% trifluoroacetic acid (TFA) (isocratic elution with 3% B for 2 min, followed by a gradient to 60% B in 6 min and isocratic elution with 95% B for 3 min). Retention time of the product (activity channel) was 6.1 min. No impurities were found, neither by radio-detection nor UV detection.

Data acquisition

All data were acquired with the PET/CT Biograph TruePoint 64 scanner (Siemens Medical Solutions, Erlangen, Germany). The PET component of this tomograph consists of four detector rings each with 48 block detectors of LSO and is a 3-D-only tomograph. The transverse field of view is 58.5 cm, while the axial field of view is extended to 21.6 cm (TrueV) leading to an 82% increase of the efficiency compared to the previous design with three detector rings. The spatial resolution at the centre of the field of view was measured as 4.4 mm. The CT component of the tomograph is a 64-slice spiral CT with a variable slice thickness of 0.6–10.0 mm and a 50-cm transverse field of view that can be extended to 70 cm by means of a fitting algorithm.

Patients were injected with 75–235 MBq ^{68}Ga-DOTA-TOC (mean 131 MBq) depending on the weight of the patient. PET data were acquired 20–28 min (average 23 min) after injection. The CT acquisition protocol included a low-dose CT (26 mAs, 120 kV, 0.5 s per rotation, 5-mm slice thickness) from the base of the skull to mid-thigh for attenuation correction with diluted oral contrast (Telebrix 300 mg) followed by the PET scan and a diagnostic CT in portal venous phase 80 s after injection of i.v. contrast agent (Imeron 300) (160 mAs, 120 kV, 0.5 s per rotation, 5-mm reconstructed slice thickness) in 27 patients. Patients were instructed to perform shallow breathing during the CT acquisition. PET data were reconstructed using an attenuation-weighted ordered subset expectation maximization (AWOSEM) algorithm; scatter and attenuation correction was performed using the CT data. Data were transferred to a Syngo TrueD workstation (Siemens Medical Solutions) for further processing.

Quantitive and qualitative assessment

At first, misalignment between CT and PET for each study was estimated by measuring the distance of the top of the liver dome in PET and CT. After manual correction for all scans with more than 1 cm misalignment between CT and PET, data origination from respiratory motion, means of the average standardized uptake values normalized to body weight (SUV_{av}) were measured for the head of the pancreas (including the hottest area), psoas muscle as reference, tail of the pancreas, liver and spleen. For liver and pancreas also the maximum standardized uptake value (SUV_{max}) was measured. SUVs were determined by generating a standardized 3-D circular region of interest with a diameter measuring 2 cm drawn on transaxial slices. In addition, SUV ratios between the head of the pancreas and liver were calculated. Statistical significance was tested with a two-tailed Student's t test; a p value<0.05 was considered as statistically significant. Non-attenuation-corrected images were reviewed side by side with attenuation-corrected images for qualitative assessment. Any noticeable uptake or no uptake in the head of the pancreas was described for every study. In case of noticeable uptake, further description as focal or diffuse was provided.

Results

Misalignment between PET and CT was noted in 23 scans (54%); mean and standard deviation of this misalignment was 1.4±1.6 cm (range 0–5.7 cm). How the magnitude of misalignment was distributed over the studies is shown in Fig. 1. The SUV in the head of the pancreas was analysed separately for the group with misalignment and without misalignment.

Among all patients, the mean and standard deviation of the SUV_{av} of the head of the pancreas was 5.8±7.6 (range 1.5–39.3), of the tail of the pancreas was 3.2±1.2 (range 1.1–6.9), of the psoas muscle was 0.6±0.2 (range 0.3–1.0), of the liver was 5.9±1.8 (range 3.2–11.9) and of the spleen was 23.8±7.4 (range 11.3–38.6). The mean and standard deviation of the SUV_{max} of the head of the pancreas was 9.8±12.5 (range 2.4–62.2) and of the liver were 7.3±1.9 (range 4.4–13.1).

Qualitative visual assessment demonstrated that 20 of 43 scans (46.6%) showed no uptake in the head of the pancreas,

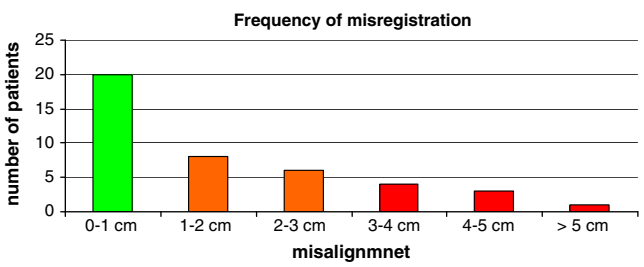

Fig. 1 Frequency of misalignment in the upper abdomen. Only 20 patients showed no noticeable misalignment (<1 cm). In the remaining 23 patients misalignment larger than 1 cm and up to 5.7 cm was found

which was classified as group 1 (Fig. 2). Of 43 scans, 23 (53.4%) showed noticeable uptake in the head of the pancreas, with focal pattern of uptake in the head of the pancreas in 10 scans (Fig. 3) and irregular pattern in 13 scans (Fig. 4).

Follow-up showed malignant pancreatic lesions in just three patients (group 3) (Figs. 5 and 6). All of these lesions have been histopathologically proven to be SSTR-positive neuroendocrine tumour. The other 20 patients with increased uptake (group 2) had no evidence of malignancy in follow-up or pathology. Quantitative data (SUV) of the three groups are shown in Table 2. Box plots of the SUV_{av} and SUV_{max} values for groups 2 and 3 are shown in Diagrams 1 and 2.

No significant difference was found between misalignment and SUVs in the pancreatic head among the different groups ($p>0.05$). Ratios between SUV_{av} in the head of the pancreas and SUV_{av} in the liver were calculated as well as the ratio between SUV_{max} in the pancreatic head and the liver for the three groups (Table 2). The pancreatic head to liver SUV_{av} ratios in case of malignancy ranged from 1.62 to 6.85, whereas these ratios ranged from 0.56 to 1.19 in case of noticeable uptake without malignancy. Considering SUV_{max}, the ratio ranged from 3.24 to 9.1 in case of malignancy compared to a ratio from 0.84 to 1.47 in case of noticeable uptake without malignancy. A ratio of 1.4 for SUV_{av} was found to be an appropriate threshold separating 100% of the malignant tumours. No statistically significant difference was noted between uptake in the head of the pancreas and liver in group 2 in both average and maximum SUVs ($p>0.05$).

Discussion

Knowledge of the biodistribution is mandatory for each clinically used radiopharmaceutical. Physiological accumulation of ^{68}Ga-DOTATOC has been described in spleen, kidneys, liver, adrenal glands, thyroid and pituitary gland [5, 9, 11]. In recent work on normal uptake and biodistribution of ^{68}Ga-DOTATOC, Boy and colleagues demonstrated that ^{68}Ga-DOTATOC imaging is related to the expression of SSTR2 at the level of mRNA in normal human tissue; moreover, they provided a novel normative database to improve the diagnosis and the treatment monitoring of sst-expressing tumours on a molecular basis [1]. Non-physiological focal ^{68}Ga-DOTATOC uptake in patients with neuroendocrine tumours should accordingly indicate possible malignancy. Gabriel and colleagues have recently reported on non-malignant or physiological ^{68}Ga-DOTATOC uptake in the head of the pancreas in 57 of 84 patients [5]. Quantification of ^{68}Ga-DOTATOC uptake in the head of the pancreas was not addressed in that study, although it might have diagnostic impact: The head of the pancreas and the closely located duodenum are typical locations for primary

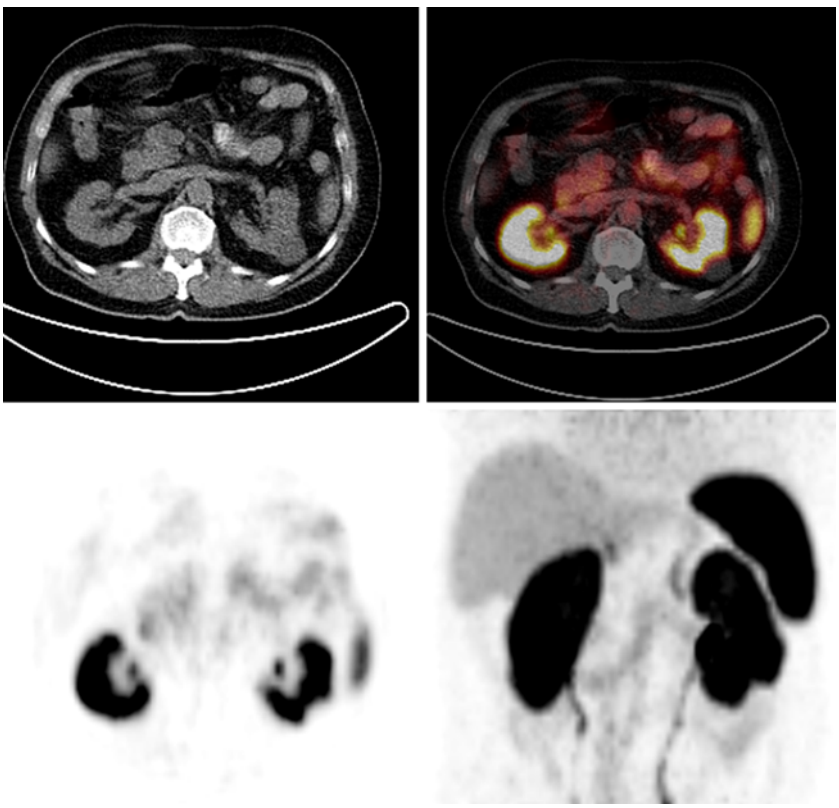

Fig. 2 No ^{68}Ga-DOTATOC uptake in the head of the pancreas could be identified

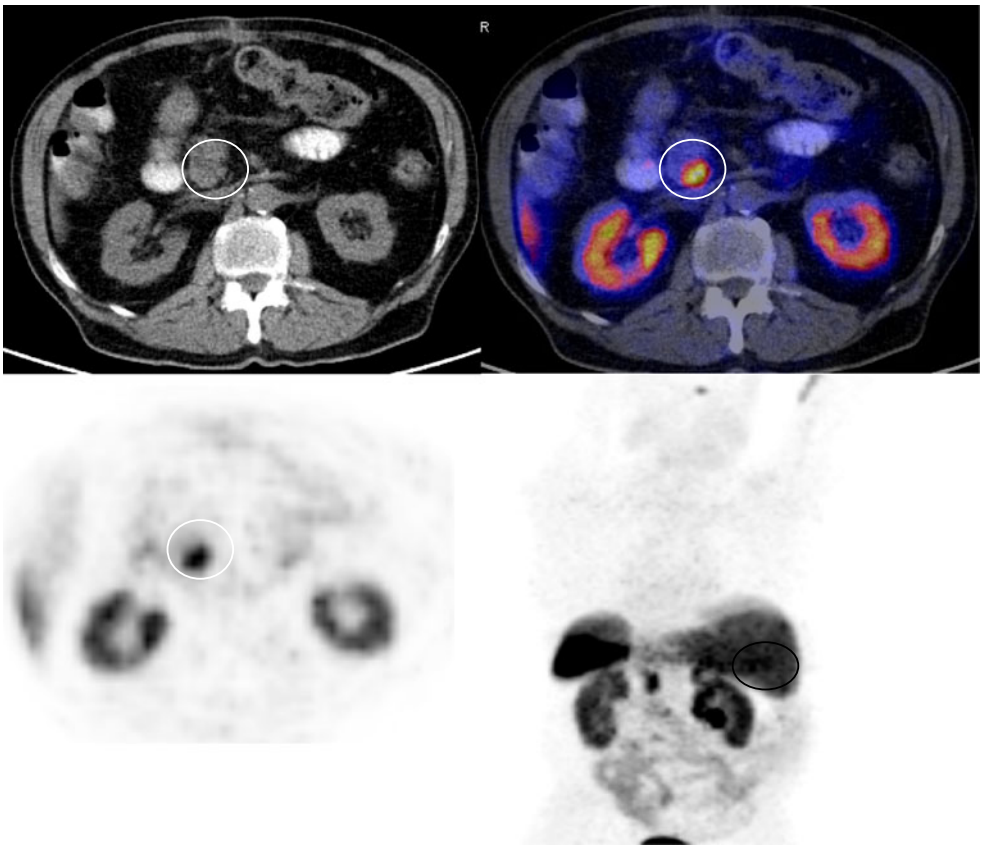

Fig. 3 Noticeable ^{68}Ga-DOTA-TOC uptake in the head of the pancreas (*circles*), SUV_{max} 7.5 and SUV_{av} 4.9; this uptake was classified as focal. SUV_{max} in the liver was 6 and SUV_{av} was 4.3. Histopathological correlation ruled out any pathological process

neuroendocrine malignancies accounting for about 8% of all neuroendocrine tumours [14].

Therefore, we quantified in this study the ^{68}Ga-DOTA-TOC uptake in the head of the pancreas. As in the

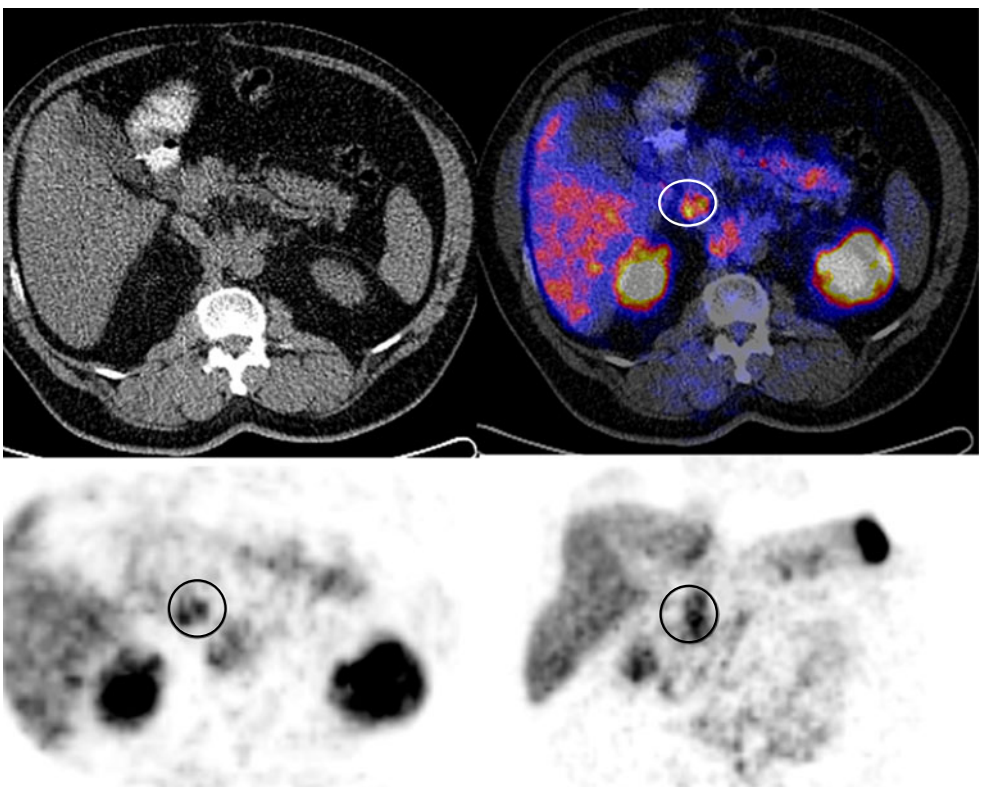

Fig. 4 Noticeable ^{68}Ga-DOTA-TOC uptake in the head of the pancreas (*circles*), SUV_{max} 6 and SUV_{av} 4.3; this uptake was classified as irregular. SUV_{max} in the liver was 5.8 and SUV_{av} was 4.8. Histopathological correlation ruled out any pathological process

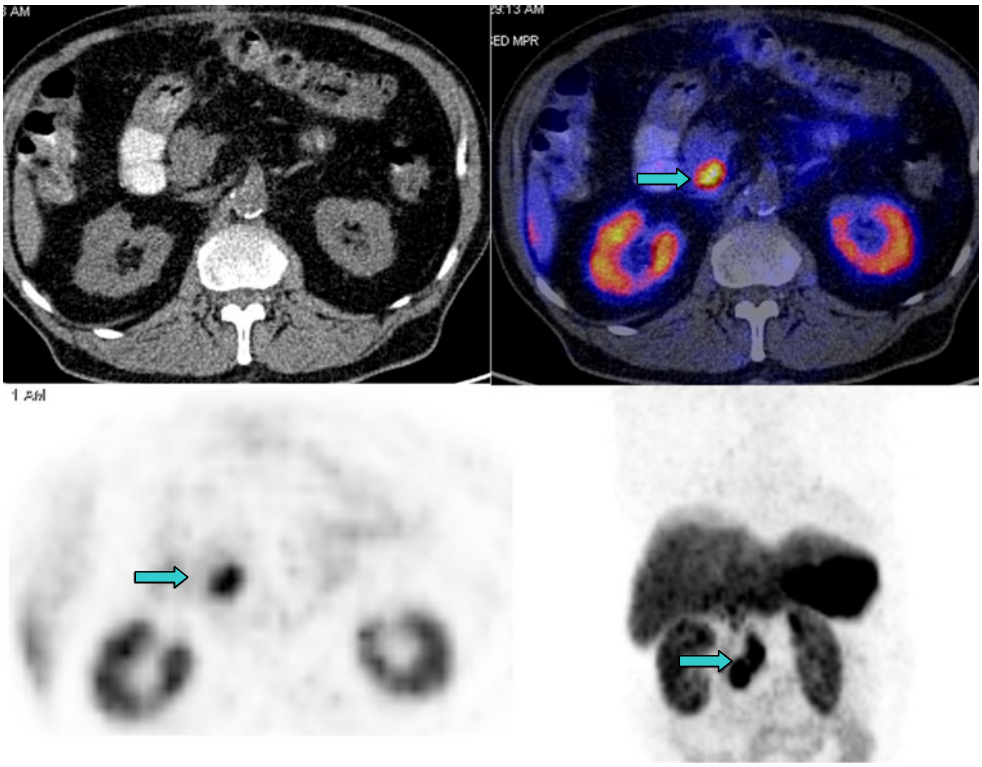

Fig. 5 Noticeable ^{68}Ga-DOTA-TOC uptake in the head of the pancreas (*arrows*), SUV_{max} 32 and SUV_{av} 12; this uptake was classified as irregular. SUV_{max} in the liver was 7.0 and SUV_{av} was 5.7. Histopathological correlation confirmed neuroendocrine tumour in the head of the pancreas

pancreatic tissue SSTR2 are expressed physiologically to a highly variable extent [16], we used in addition to the absolute uptake the ratio to the liver, also expressing SSTR2 physiologically.

Visual analysis of the PET/CT images showed that misalignment of PET and CT data is a common problem in the area of the upper abdomen [4]. In the present study, in 49% of the scans misalignment of the liver dome, considered to have an influence on the diagnosis in the pancreatic area, was found. The reason for this were different breathing states in corresponding CT and PET acquisitions, although patients were instructed to perform shallow breathing during CT which was found to be optimal by Goerres et al. [6]. However, this result indicates that better patient preparation and perhaps training of the technicians is necessary to reduce the extent of misalignment. Respiratory gating of the PET images [15] may also help to reduce misalignment as for the image fusion the optimal

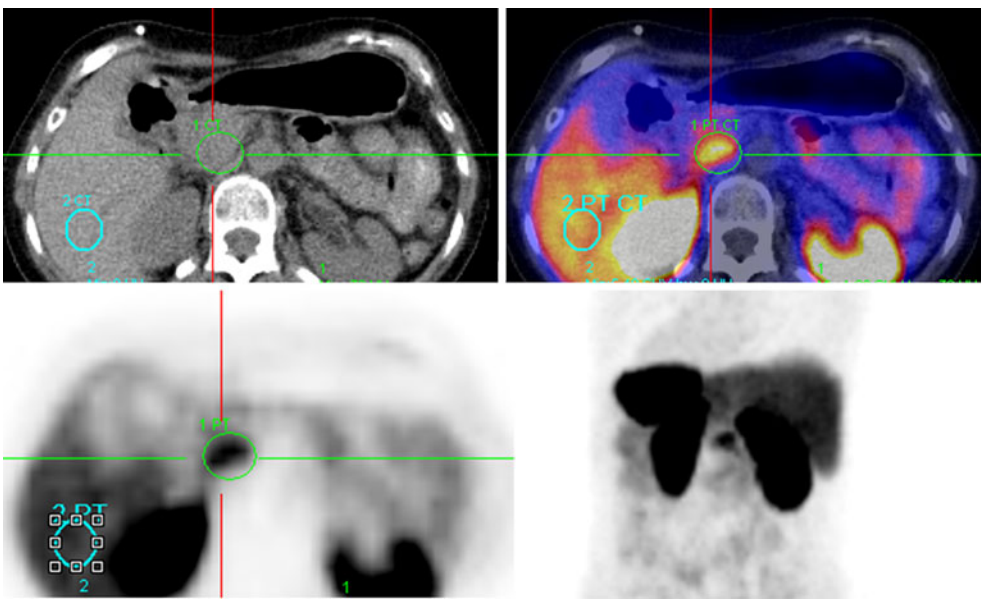

Fig. 6 Noticeable ^{68}Ga-DOTA-TOC uptake in the head of the pancreas (*arrows*), SUV_{max} 56 and SUV_{av} 37; this uptake was classified as focal. SUV_{max} in the liver was 8 and SUV_{av} was 6. Histopathological correlation confirmed neuroendocrine tumour in the head of the pancreas

Table 2 Results for SUV and SUV ratios for the three different groups

	Group 1	Group 2	Group 3
Uptake configuration	No visual uptake	Noticeable uptake without malignancy	Noticeable uptake with malignancy
Number of studies	20	20	3
Focal uptake	0	8	2
Irregular uptake	0	12	1
Mean SUV_{av} in head of pancreas ± SD (range)	2.8±0.6 (1.5–3.9)	5.5±1.5 (3.6–8.7)	29.7±15.1 (12.2–39.4)
Mean SUV_{av} in liver ± SD (range)	5.4±1.4 (3.3–8.7)	6.2±2.2 (3.8–11.9)	6.5±1.0 (5.8–7.6
Ratio of SUV_{av} pancreatic head to liver ± SD (range)	0.5±0.2 (0.2–0.8)	0.9±0.2 (0.6–1.2)	4.9±2.8 (1.6–6.9)
Mean SUV_{max} in head of pancreas ± SD (range)	4.0±0.8 (2.4–5.3)	9.3±3.1 (5.5–15.5)	51.6±15.7 (34.1–64.2)
Mean SUV_{max} in liver ± SD (range)	6.6±1.2 (4.8–9.1)	7.8±2.2 (4.6–13.2)	8.5±1.8 (7.0–10.5)
Ratio of SUV_{max} pancreatic head to liver ± SD (range)	0.6±0.2 (0.3–1.1)	1.2±0.2 (1.6–6.9)	6.5±3.0 (3.2–9.1)

PET frame can be used. However, if doing respiratory gated PET the acquisition time of the PET data must be increased which is often not practicable due to workflow issues or patient comfort or a reduced image quality must be taken into account. To avoid overlapping activity from adjacent structures, e.g. bowel wall, into the head of the pancreas due to misalignment, pre-measurement corrections can be performed using the organ border, e.g. the liver, as landmarks. This option which does not need additional scan time and can be performed in most commercial PET/CT software systems was applied in our study.

For quantification, both SUV_{max} and SUV_{av} were chosen, as SUV_{max} is observer independent, but SUV_{av} is more robust against statistical differences in SUVs [8]. The analysed PET findings were generally small, so the use of SUV_{av} alone appeared not to be sufficient for analysis, because otherwise voxels without enhanced activity might wrongly decrease SUV_{av}.

With 53.4% of all studies (23/43), enhanced ^{68}Ga-DOTATOC uptake in the head of the pancreas is quite common; 20 of these 23 patients (group 2), however, showed an uptake, which was not significantly different from uptake in the liver (Table 2). For comparison, we introduced the ratio between the uptake in the head of the pancreas and the liver, for both SUV_{max} and SUV_{av}, which were correspondingly close to 1. The remaining 3 of the 23 patients (group 3) showed pancreatic uptake much higher than the liver uptake with ratios of 4.9±2.8 (SUV_{av}) and 6.5±3.0 (SUV_{max}), respectively.

In such a typical clinical setting as the one presented here, histological verification is not available as the 'gold standard' for most of the patients. However, we studied consecutive patients with an indication for a ^{68}Ga-DOTA-TOC PET independent of clinical history, especially not just patients with a dedicated question of pancreatic lesions, e.g. search for primaries. In addition, the clinical follow-up was relatively long lasting with at least 6 and up to 20 months depending on specific markers and radiological imaging (CT and ^{68}Ga-DOTATOC PET). In six patients who underwent two consecutive scans in this study, three patients had fixed pattern as no uptake, irregular benign uptake and focal benign uptake, another two patients had variable pattern from no uptake to irregular benign uptake and the last patient had variable from irregular benign pattern to focal benign pattern. Only patients after pancreatic surgery or local radiation therapy were not included in this study, as they mostly show an altered anatomical situs; additionally, a higher prevalence of malignancy can

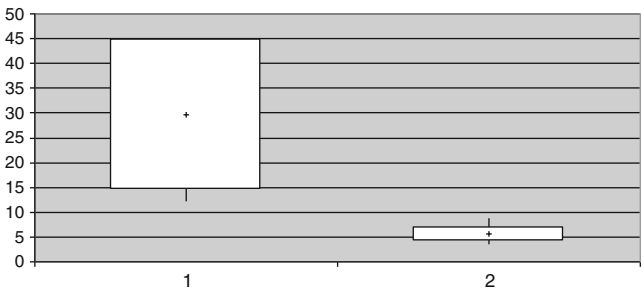

Diagram 1 SUV_{av} in the group with proven malignancy (*1*) and the group with uptake in the head of the pancreas but without evidence of malignancy (*2*)

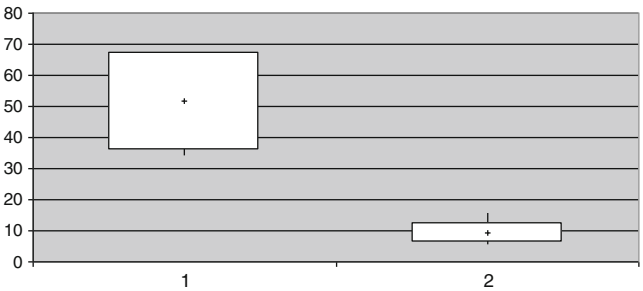

Diagram 2 SUV_{max} in the group with proven malignancy (*1*) and the group with uptake in the head of the pancreas but without evidence of malignancy (*2*)

be found in these patients. Patients with extensive liver metastases, relatively common in neuroendocrine tumours, were excluded, as calculation of the uptake in these patients may be influenced by spillover of activity from the liver metastases into the volume of the pancreas.

Based on the criteria defined before, just three patients (group 3) had had proven malignancy in the head of the pancreas (Figs. 5 and 6) with expression of SSTR2. The ratio of pancreatic DOTATOC uptake to the liver uptake turned out to be the best parameter to differentiate between group 2 and group 3, which means separation between malignant tumour in the head of the pancreas and physiological hepatobiliary and intestinal excretion of the radiotracer in this area (Diagrams 1 and 2). We found a ratio of the SUV_{av} of 1.4 to separate malignant from physiological uptake in our patients. However, due to the low number of patients showing malignancies this threshold cannot be used in general, and a larger number of patients must therefore be evaluated. Lesion to reference organ ratios were also used by Hofmann et al. [9]. They reported on tumour to non-tumour ratios for ^{68}Ga-DOTATOC uptake ranging from 100:1 for CNS to just >3:1 for liver, the latter well comparable to our result of 4.9 for this ratio. Buchmann and colleagues reported on hepatic tumour to non-tumour ratios on ^{68}Ga-DOTATOC PET ranging from 1.3 to 4.9, indicating that tumour uptake in neuroendocrine tumours is in general higher than the normal liver uptake [3]. Also Gabriel and colleagues [5] found tumour uptake in the liver and the abdomen to be higher than physiological liver uptake. They described also uptake in the pancreatic head without known pathology in 68% of their patients, but did not perform quantification in this area. The only case designated as false-positive in this prospective study was reported in the head of the pancreas.

A minor limitation of this study is the relatively small number of patients with proven malignant findings in the head of the pancreas, which hinders comparative statistical analysis. Though the differences of pancreatic head to liver ratios in both SUV_{av} and SUV_{max} between group 2 and group 3 were significant, the small number of patients and the large tumour size in two of three patients of group 3 make a general conclusion unreliable. Nevertheless, this kind of quantification is likely to become a helpful tool for differentiation between benign and malignant tissue.

Conclusion

^{68}Ga-DOTATOC uptake in the head of the pancreas is a common finding in patients undergoing ^{68}Ga-DOTATOC PET/CT. Based on the results of our study, such uptake most likely does not represent a malignant process, if the ratio to the liver uptake is around 1. Therefore, quantification is recommended to avoid a false-positive diagnosis in this clinically relevant location for neuroendocrine tumours. In our patient cohort a threshold of 1.4 for the ratio of SUV_{av} in the head of the pancreas and the liver was found to separate malignant from benign findings, but such a threshold must be evaluated in a larger number of patients. As misalignment between CT and PET data was found in 54% of the studies, respiratory movement has to be taken into account by careful analysis of the native images and their adequate correction.

Conflicts of interest None.

References

1. Boy C, Heusner TA, Poeppel TD, Redmann-Bischof A, Unger N, Jentzen W, et al. (68)Ga-DOTATOC PET/CT and somatostatin receptor (sst1-sst5) expression in normal human tissue: correlation of sst2 mRNA and SUV(max). Eur J Nucl Med Mol Imaging 2011;38:1224–36. doi:10.1007/s00259-011-1760-x.
2. Brandner ED, Wu A, Chen H, Heron D, Kalnicki S, Komanduri K, et al. Abdominal organ motion measured using 4D CT. Int J Radiat Oncol Biol Phys 2006;65(2):554–60.
3. Buchmann I, Henze M, Engelbrecht S, Eisenhut M, Runz A, Schäfer M, et al. Comparison of 68Ga-DOTATOC PET and 111In-DTPAOC (Octreoscan) SPECT in patients with neuroendocrine tumours. Eur J Nucl Med Mol Imaging 2007;34(10):1617–26.
4. Bundschuh RA, Martinez-Möller A, Ziegler SI, Schwaiger M, Scheidhauer K. Misalignment in PET/CT: relevance for SUV and therapy management. Nuklearmedizin 2008;47(2):N14–5.
5. Gabriel M, Decristoforo C, Kendler D, Dobrozemsky G, Heute D, Uprimny C, et al. 68Ga-DOTA-Tyr3-octreotide PET in neuroendocrine tumors: comparison with somatostatin receptor scintigraphy and CT. J Nucl Med 2007;48:508–18.
6. Goerres GW, Kamel E, Seifert B, Burger C, Buck A, Hany TF, et al. Accuracy of image coregistration of pulmonary lesions in patients with non-small cell lung cancer using an integrated PET/CT system. J Nucl Med 2002;43(11):1469–75.
7. Haug A, Auernhammer CJ, Wängler B, Tiling R, Schmidt G, Göke B, et al. Intraindividual comparison of 68Ga-DOTA-TATE and 18F-DOPA PET in patients with well-differentiated metastatic neuroendocrine tumours. Eur J Nucl Med Mol Imaging 2009;36:765–70. doi:10.1007/s00259-008-1030-8.
8. Hermann K, Krause BJ, Bundschuh RA, Dechow T, Schwaiger M. Monitoring response to therapeutic interventions in patients with cancer. Semin Nucl Med 2009;39(3):210–32.
9. Hofmann M, Maecke H, Börner R, Weckesser E, Schöffski P, Oei L, et al. Biokinetics and imaging with the somatostatin receptor PET radioligand (68)Ga-DOTATOC: preliminary data. Eur J Nucl Med 2001;28:1751–7.
10. Koukouraki S, Strauss LG, Georgoulias V, Eisenhut M, Haberkorn U, Dimitrakopoulou-Strauss A. Comparison of the pharmacokinetics of 68Ga-DOTATOC and [18F]FDG in patients with metastatic neuroendocrine tumours scheduled for 90Y-DOTATOC therapy. Eur J Nucl Med Mol Imaging 2006;33(10):1115–22. Epub 2006 Jun 9.
11. Kowalski J, Henze M, Schuhmacher J, Maecke HR, Hofmann M, Haberkorn U. Evaluation of positron emission tomography imaging using [68Ga]-DOTA-D-Phe(1)-Tyr(3)-octreotide in comparison to [111In]-DTPAOC SPECT. First results in patients with neuroendocrine tumors. Mol Imaging Biol 2003;5:42–8.
12. Kumar U, Sasi R, Suresh S, Patel A, Thangaraju M, Metrakos P, et al. Subtype-selective expression of the five somatostatin receptors

(hSSTR1–5) in human pancreatic islet cells: a quantitative double-label immunohistochemical analysis. Diabetes 1999;48(1):77–85.
13. Meisetschläger G, Poethko T, Stahl A, Wolf I, Scheidhauer K, Schottelius M, et al. Gluc-Lys([18F]FP)-TOCA PET in patients with SSTR-positive tumors: biodistribution and diagnostic evaluation compared with [111In]DTPA-octreotide. J Nucl Med 2006;47 (4):566–73.
14. Modlin IM, Lye KD, Kidd M. A 5-decade analysis of 13,715 carcinoid tumors. Cancer 2003;97(4):934–50.
15. Nehmeh SA, Erdi YE, Ling CC, Rosenzweig KE, Schoder H, Larson SM, et al. Effect of respiratory gating on quantifying PET images of lung cancer. J Nucl Med 2002;43(7):876–81.
16. Reubi JC, Waser B, Schaer JC, Laissue JA. Somatostatin receptor sst1-sst5 expression in normal and neoplastic human tissues using receptor autoradiography with subtype-selective ligands. Eur J Nucl Med 2001;28(7):836–46.
17. Stahl A, Meisetschläger G, Schottelius M, Bruus-Jensen K, Wolf I, Scheidhauer K, et al. [123I]Mtr-TOCA, a radioiodinated and carbohydrated analogue of octreotide: scintigraphic comparison with [111In]octreotide. Eur J Nucl Med Mol Imaging 2006;33 (1):45–52.
18. Win Z, Al-Nahhas A, Rubello D, Gross MD. Somatostatin receptor PET imaging with gallium-68 labeled peptides. Q J Nucl Med Mol Imaging 2007;51(3):244–50.